

Figure 1. Zn-(DL)DTT (\blacklozenge); Cd-(DL)DTT (\blacksquare); Ni-(DL)DTT (\blacktriangle); Mn-(DL)DTT (\times).

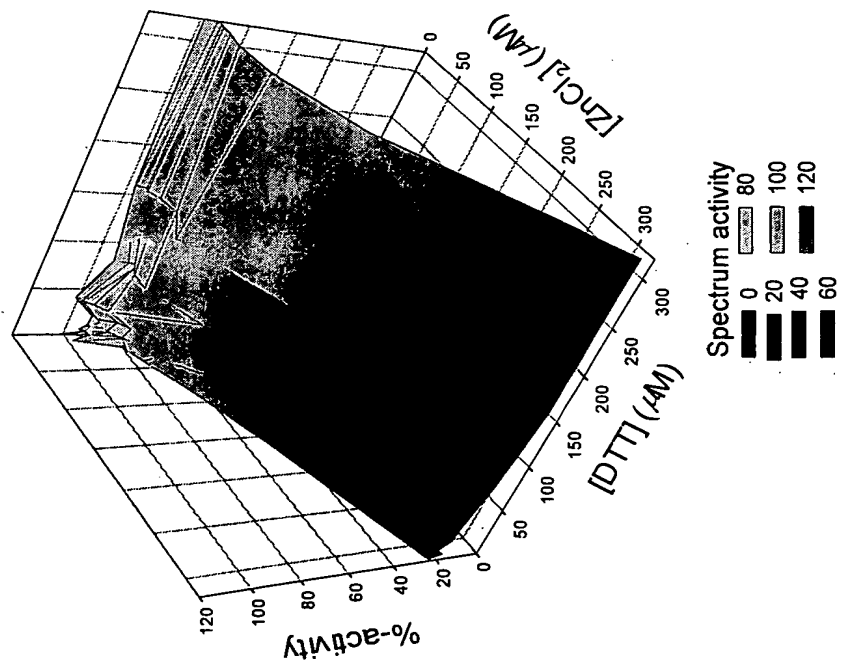


Figure 2A.

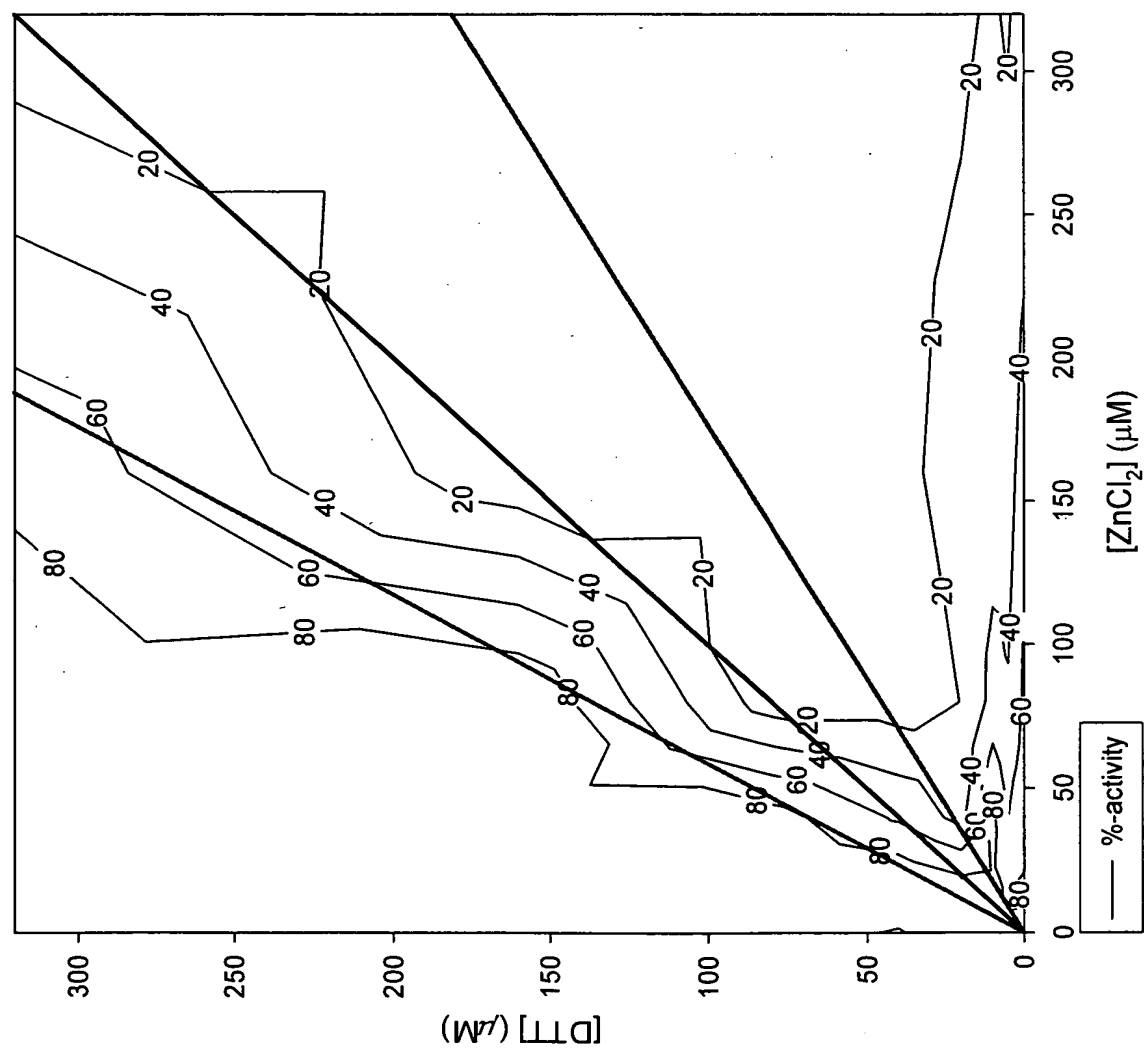


Figure 2B.

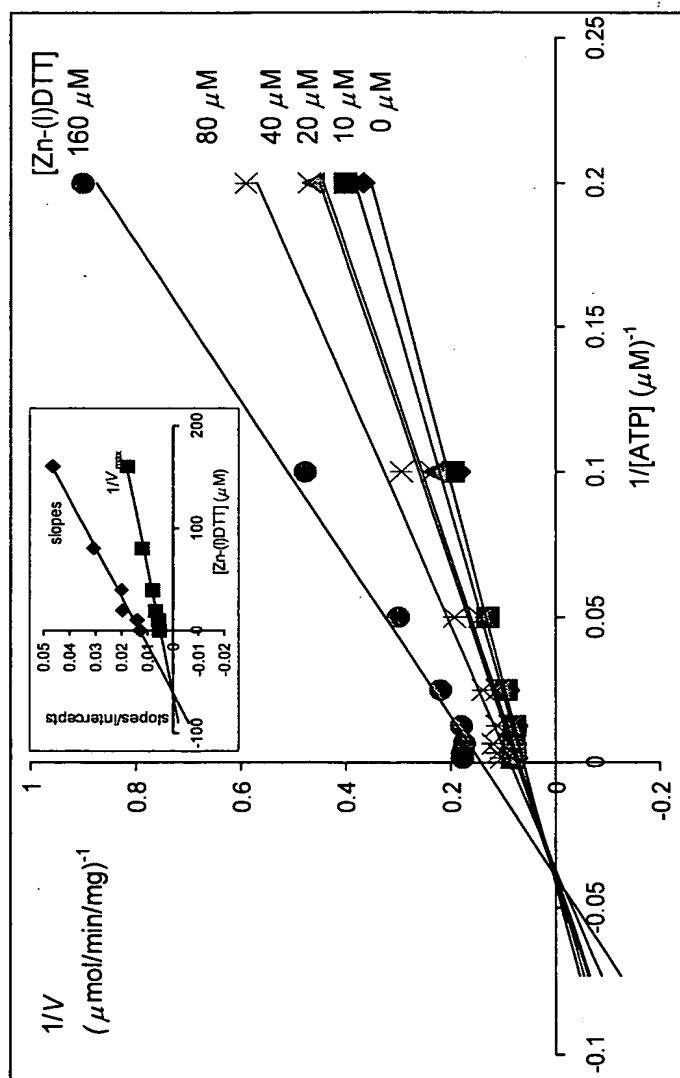


Figure 3A. Inset, a plot of the slopes (\diamond) and intercepts (\blacksquare) versus Zn-(L)DTT concentrations.

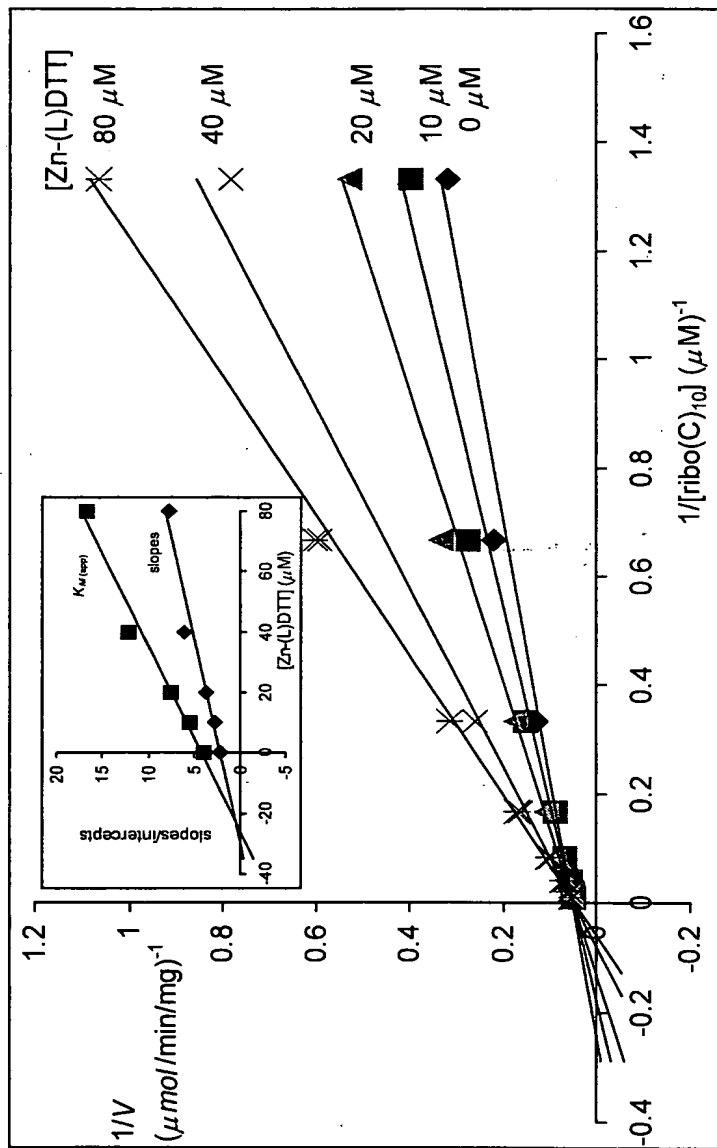


Figure 3B. Inset, a plot of the slopes (\diamond) and intercepts (\blacksquare) versus Zn-(L)DTT concentrations.

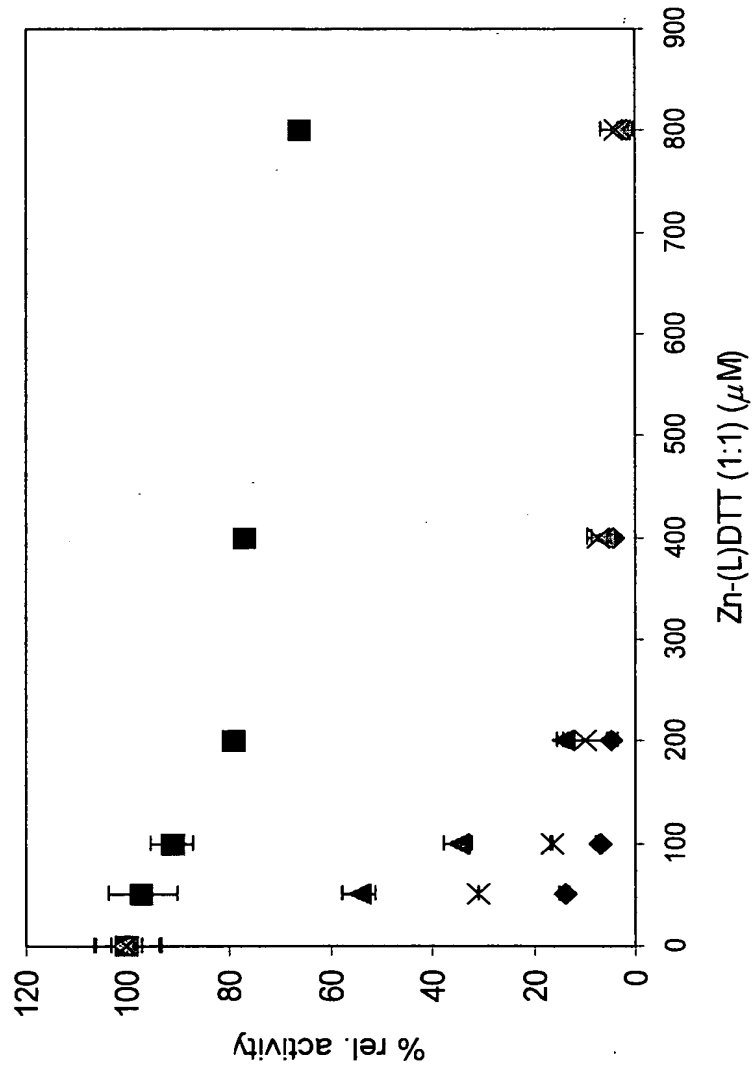


Figure 4. Control (♦); no preincubation (■); 10-fold concentration of rho, poly(C) and ATP (▲); standard condition + 0.1 mg/mL BSA (×).

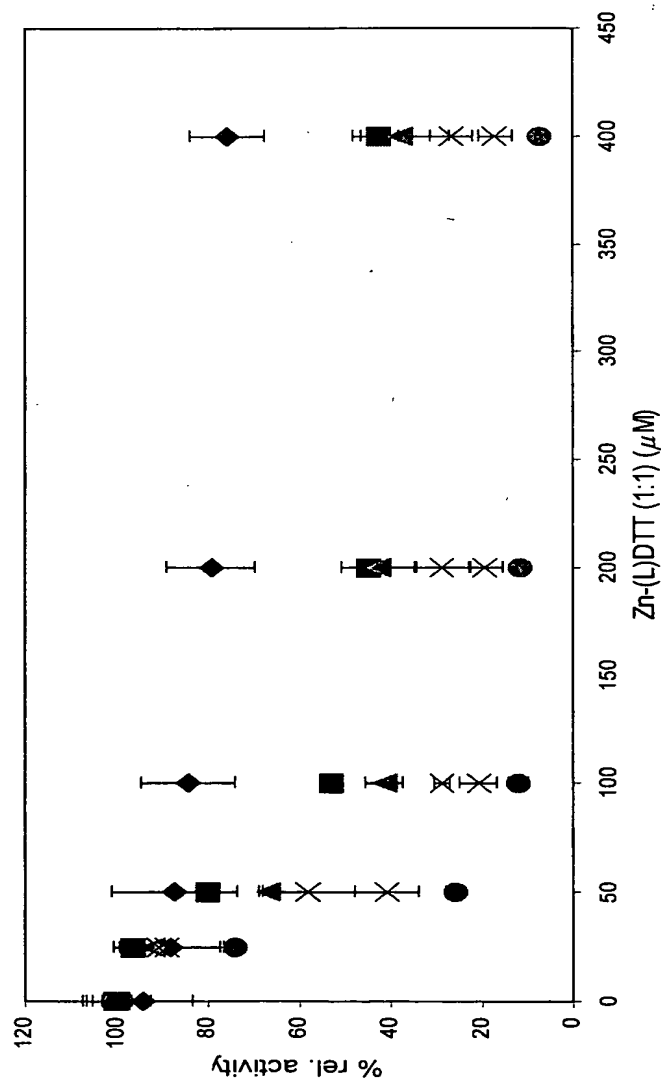


Figure 5. No preincubation (\blacklozenge); 15 sec (\blacksquare); 30 sec (\blacktriangle); 1 min (\times); 2 min (\times); 5 min (\bullet).

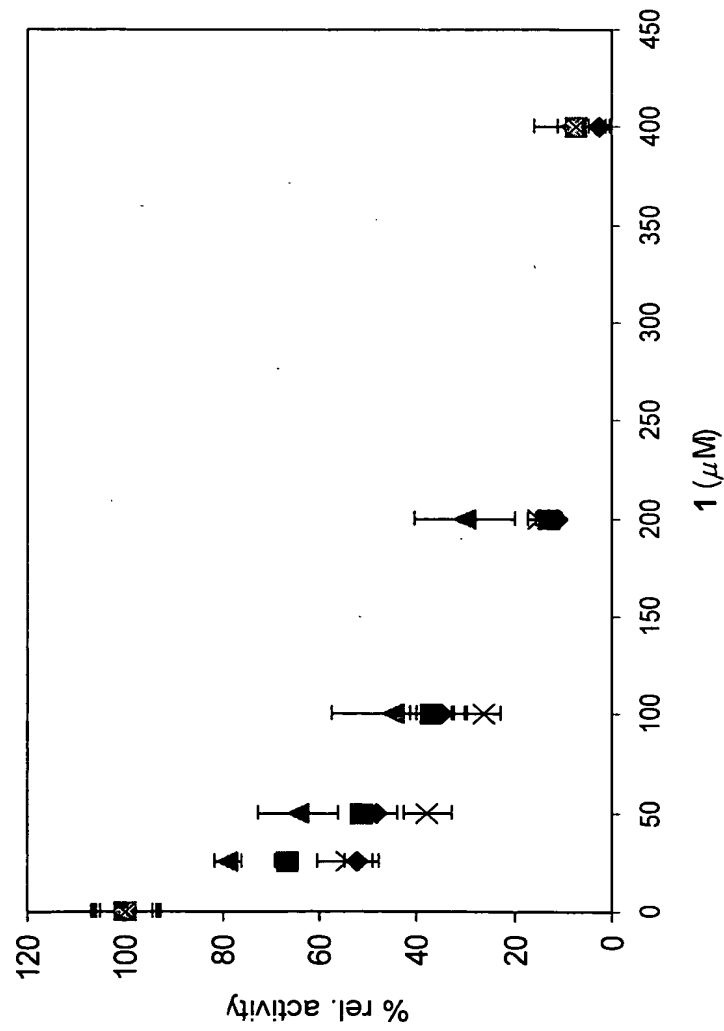


Figure 6. Control (♦); No preincubation (■); 10-fold concentration of rho, poly(C) and ATP (▲); standard condition + 0.1 mg/mL BSA (X).

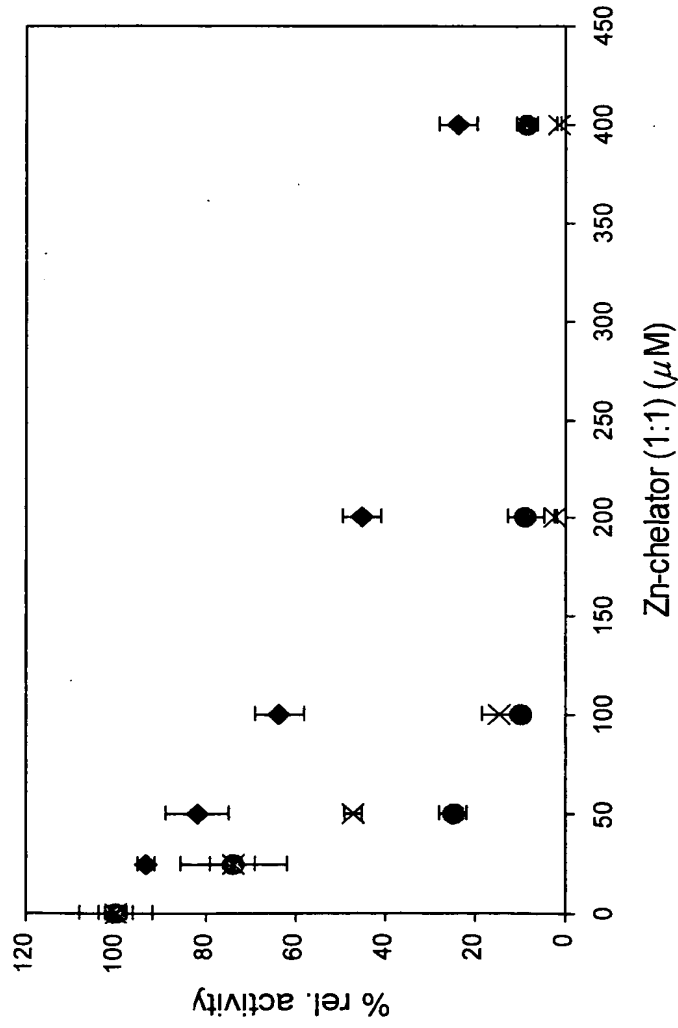


Figure 7. Zn-2-mercaptoethanol (♦); Zn-1,2-ethanedithiol (X); Zn-(L)DTT (•).

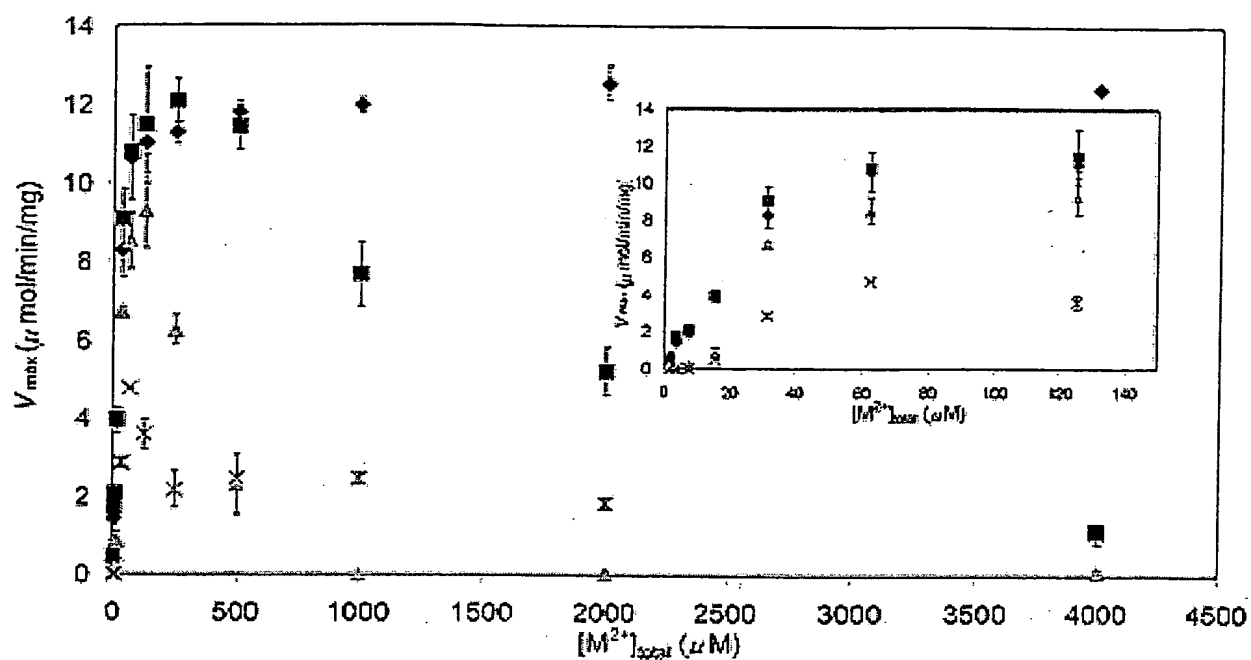


Figure 8. The average velocities of two determinations are plotted with Mg^{2+} (diamonds), Mn^{2+} (squares), Zn^{2+} (gray triangles), and Cd^{2+} (x). The inset shows metal activation of rho exhibiting a peak velocity and sigmoidal behavior at rho divalent metal concentrations.